



Cite this: *Chem. Commun.*, 2022, **58**, 5273

Received 28th December 2021,  
Accepted 1st April 2022

DOI: 10.1039/d1cc07265j

[rsc.li/chemcomm](http://rsc.li/chemcomm)

## Controlled polymerization of metal complex monomers – fabricating random copolymers comprising different metal species and nano-colloids†

Shigehito Osawa, <sup>a,b</sup> Sosuke Kurokawa<sup>c</sup> and Hidenori Otsuka <sup>a,b,c</sup>

Acrylate monomers with metal complexes were designed to build polymer metal complexes. The ideal copolymerization of monomers with zinc and platinum was performed to obtain random copolymers with a feeding metal composition. The successful nano-colloid preparation from the polymers further highlighted the potential of the method for building multimetallic materials.

Hybrid materials with organic and inorganic components have attracted increasing attention.<sup>1–4</sup> Polymers with metal complexes on side chains are very promising as high-performance hybrid materials because they enable in-solution locally concentrated states of the metal complexes to remain as secondary valence sites, with better catalytic activity and molecular recognition.<sup>5–8</sup> Because the electron density-dependent properties of metal complexes are affected by their molecular neighborhood, grafting polymer complexes with different metal species can further widen the scope of polymer applications.<sup>9,10</sup> In general, the incorporation of metal complexes into the side chains is accomplished by mixing metal species with ligand-structured polymers (Scheme 1a).<sup>5,6,11,12</sup> However, this process is not suitable for preparing polymer chains that incorporate types of complexes with different metal species. It is difficult to control the metal components on the polymer chains by simply changing the feeding metal compositions to the polymer, because the ligand-binding affinity varies across metal species. Thus, a well-conceived approach is required to obtain the desired metal composition in the polymer chains.

<sup>a</sup> Department of Applied Chemistry, Faculty of Science, Tokyo University of Science, Kagurazaka 1-3, Shinjuku-ku, Tokyo, 162-8601, Japan

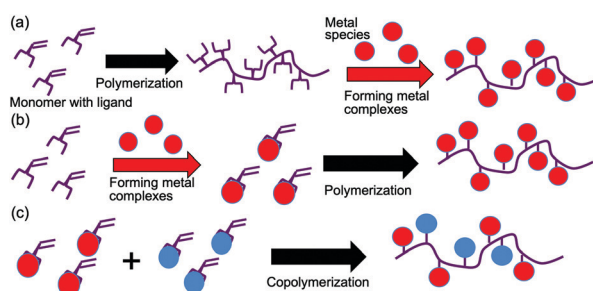
E-mail: [osawa-s@rs.tus.ac.jp](mailto:osawa-s@rs.tus.ac.jp), [h.otsuka@rs.tus.ac.jp](mailto:h.otsuka@rs.tus.ac.jp)

<sup>b</sup> Water Frontier Research Center (WaTUS), Research Institute for Science and Technology, Tokyo University of Science 1-3 Kagurazaka, Shinjuku-ku, Tokyo, 162-8601, Japan

<sup>c</sup> Department of Chemistry, Graduate School of Science, Tokyo University of Science, Kagurazaka 1-3, Shinjuku-ku, Tokyo, 162-8601, Japan

† Electronic supplementary information (ESI) available: Materials and methods of the experiments, monomers' characterization, and <sup>1</sup>H NMR spectra of the polymerization mixtures and obtained polymers. See <https://doi.org/10.1039/d1cc07265j>

Herein, we focus on the preparation of polymers with metal complexes using monomers composed of metal complexes and a polymerizing group (Scheme 1b), which have been used to obtain polymers with metallocene and metallocenophanes.<sup>13,14</sup> This approach differs from the widely adopted procedure, in which a polymer backbone with a ligand structure is prepared before the formation of metal complexes (Scheme 1a).<sup>5,6,11,12</sup> Notably, this approach achieved the synthesis of polymer chains containing two metal species in the polymer backbone by polymerizing monomers containing two metal species.<sup>15</sup> In this case, metal species along the polymer backbone can be fabricated in an ideal alternating manner. However, the preparation of a single monomer that contains two metal motifs is challenging. In this study, we assumed that the co-polymerization of monomers with different metal species could be used to build polymers incorporating complexes with different metal species in a controlled manner, which would be a much simpler synthetic procedure. It is expected that the monomer feeding molar ratio would regulate the metal composition of the resulting copolymers when no free metal ions remained in the polymerization mixture (Scheme 1c). In this strategy, selecting a ligand structure with good chelation properties was the key to designing monomers with metal complexes. In this study, we selected dipicolylamine (DPA) as the ligand structure because it is



**Scheme 1** Preparation of metal complex-pendent polymer chain: (a) widely performed procedure, (b) proposed procedure, and (c) outreach procedure for obtaining polymers in complex with different metal species at controlled ratio.



a tridentate ligand with good chelation properties for various metal species.<sup>16,17</sup> It should be further noted that DPA is an excellent metal ligand that has been used in various biochemical applications, including apoptosis detection reagents and gene carriers.<sup>18,19</sup> In this study, we designed a DPA acrylate (DPAAc) monomer and formed metal complexes with it. The designed monomers were polymerized or co-polymerized *via* reversible addition-fragmentation chain transfer (RAFT) polymerization to construct polymer chains with metal complexes.

We previously reported the RAFT polymerization of DPA methacrylate (DPAMA).<sup>5</sup> Note that we selected DPAAc instead of DPAMA as the monomer structure in this study because the slower and lower consumption of this monomer is beneficial for controlling and characterizing random copolymerization in terms of Fineman–Ross plots, which are used below to evaluate the copolymerization behavior of DPAAc complexes with different metal species. When the DPAAc polymerization was traced using <sup>1</sup>H nuclear magnetic resonance (<sup>1</sup>H NMR) spectra by monitoring the consumption of acrylate groups (*i.e.*, monomer conversion), the DPAAc exhibited lower monomer conversion compared with that previously reported for DPAMA. The monomer conversions were approximately 10% and 70% for DPAAc (Fig. 1e) and DPAMA,<sup>5</sup> respectively, after 48 h of reaction.

To verify that DPAAc metal complexes could be polymerized, DPAZn(II)Ac was polymerized *via* RAFT polymerization. DPA has been reported to form a complex with zinc in a chemically stoichiometric ratio.<sup>18,19</sup> As shown in Fig. 1a and b, the proton signals derived from the pyridine group of DPAAc were shifted when zinc chloride was added in the same molar amount as DPAAc, indicating the successful formation of DPAZn(II)Ac. During the polymerization reaction, 49% of the DPAZn(II)Ac monomer was consumed over 48 h (Fig. 1e), confirming that the metal complex monomers of DPAZn(II)Ac could be polymerized. Interestingly, the DPAAc conversion was accelerated by forming complexes with zinc, whereas the conversion of the DPAAc monomer reached 9% after 12 h, after which it plateaued. Presumably, the pyridyl groups in DPA could exhibit steric hindrance, which could disturb the polymerization reaction, and the formation of coordination bonds with Zn(II) could reduce the mobility of the pyridyl groups and their steric hindrance. The obtained pDPAZn(II)Ac was evaluated using gel permeation chromatography (GPC) after removing Zn(II) by dialysis against methanol containing an excess amount of diethylenetriamine as a chelating agent. The obtained polymer exhibited a unimodal peak with a molecular weight distribution of 2.173 for *D*, based on the polyethylene glycol (PEG) standard, further confirming that the polymerization was successful. Notably, adding water to the polymerization solvent (*i.e.*, changing the solvent from DMF to DMF (80% v/v)/water (20% v/v)) improved the polymerization of DPAZn(II)Ac and reduced the molecular weight distribution of the resultant polymers. The monomer conversion after 48 h slightly increased to 56%, and *D* improved to 1.704 (Fig. 1f). This may have been due to the improved solubility of the monomers and polymers in the polymerization solvent. Finally, DMF (80% v/v)/water (20% v/v) was selected as the polymerization solvent.

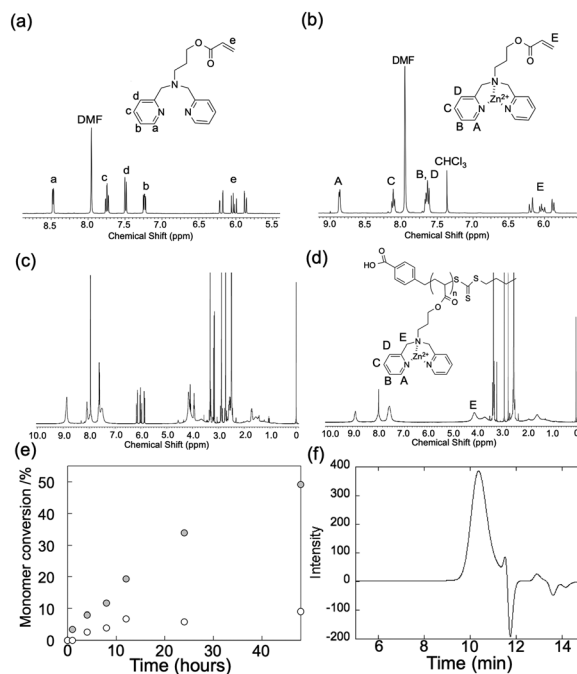


Fig. 1 Characterization of DPAZn(II)Ac polymerization. <sup>1</sup>H NMR spectra of the (a) DPAAc, (b) DPAZn(II)Ac, and (c) representative DPAZn(II)Ac polymerization mixtures to determine monomer conversion, as well as that of (d) the obtained pDPAZn(II)Ac. (e) The time courses of the DPAZn(II)Ac (gray) and DPAAc (white) monomer conversion percentages. (f) GPC curves for the obtained polymer after zinc removal by dialysis against methanol with excess amount of diethylenetriamine.

The polymerization of other metal complexes with DPAAc was then performed. In this study, we investigated the polymerization of the Pt(II) complex with DPAAc, because platinum forms metal complexes with DPA in a chemically stoichiometric manner, and these metal complexes are advantageous for biomedical and electronic applications.<sup>20,21</sup> The polymerization reaction was facilitated for DPAPt(II)Ac, similar to that for DPAZn(II)Ac, and the monomer conversion was 50% after 48 h, as determined by <sup>1</sup>H NMR measurements (Fig. S4, ESI†).

Subsequently, we performed the copolymerization of DPAZn(II)Ac and DPAPt(II)Ac to demonstrate the possibility of controlling the metal composition of the polymer chain by regulating the monomer feeding ratio. Notably, bimetallic materials composed of platinum and zinc have attracted increasing attention as catalytic materials with better performance than pure platinum and zinc materials.<sup>22,23</sup> The signals of the pyridine groups of DPAAc in the <sup>1</sup>H NMR spectra for the complexes with Zn(II) and Pt(II) could be distinguished (Fig. 2b, d, and Fig. S5, ESI†). Thus, the copolymerization behavior of these monomers could be traced by monitoring the signals in the <sup>1</sup>H NMR spectra. Both monomers were equally consumed, regardless of the molar ratio of DPAZn(II)Ac/DPAPt(II)Ac (Table 1). Based on these results, we further estimated monomer reactivity ratios *r*<sub>1</sub>, which indicated the relative reactivity of DPAZn(II)Ac to DPAPt(II)Ac when the growing polymer end was DPAZn(II)Ac, and *r*<sub>2</sub>, which indicated the relative reactivity of DPAPt(II)Ac to DPAZn(II)Ac when the growing polymer end was DPAPt(II)Ac. By adjusting the Mayo–Lewis equation<sup>24</sup> the monomer concentrations (*i.e.*, [DPAZn(II)Ac] and [DPAPt(II)Ac]) determined the

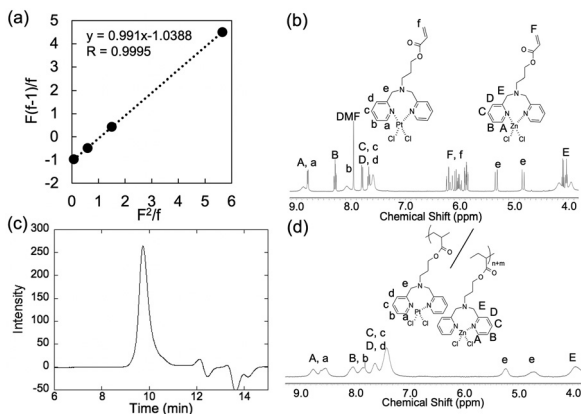


Fig. 2 Characterization of DPAZn(II)Ac and DPAPt(II)Ac co-polymerization. (a) Fineman–Ross plot of the DPAZn(II)Ac and DPAPt(II)Ac co-polymerization. (b)  $^1\text{H}$  NMR spectra of the polymerization mixture for Zn1/Pt1. (c) GPC curve of the obtained Zn1/Pt1, after removing zinc and platinum ions by dialysis against methanol with excess ethylenediamine. (d)  $^1\text{H}$  NMR spectra of Zn1/Pt1.

monomer consumption speeds (*i.e.*,  $d[\text{DPAZn(II)Ac}]$  and  $d[\text{DPAPt(II)Ac}]$ ), as follows.

$$\frac{d[\text{DPAZn(II)Ac}]}{d[\text{DPAPt(II)Ac}]} = \frac{[\text{DPAZn(II)Ac}]}{[\text{DPAPt(II)Ac}]} \times \frac{r_1[\text{DPAZn(II)Ac}] + [\text{DPAPt(II)Ac}]}{[\text{DPAZn(II)Ac}] + r_2[\text{DPAPt(II)Ac}]} \quad (1)$$

Subsequently, this equation was transformed by assigning  $f$  and  $F$  to  $d[\text{DPAZn(II)Ac}]/d[\text{DPAPt(II)Ac}]$  and  $[\text{DPAZn(II)Ac}]/[\text{DPAPt(II)Ac}]$ , respectively, to determine  $r_1$  and  $r_2$  using the Fineman–Ross method.<sup>25</sup>

$$F(f-1) = \frac{F^2}{f}r_1 - r_2. \quad (2)$$

In this estimation, we denote the DPAZn(II)Ac/DPAPt(II)Ac ratio in the obtained polymer by  $f$ , while the DPAZn(II)Ac/DPAPt(II)Ac ratio in the polymerization mixture at the beginning is denoted by  $F$ , assuming that the monomer reaction conditions do not significantly change during the reactions because the monomer conversion percentages are 12.6–16.8% (Table 1). Then, a Fineman–Ross plot was constructed based on the calculated values of  $F(f-1)/F$  and  $F^2/f$  (Table 1), eventually determining that reactivity ratios  $r_1$  and  $r_2$  were 0.991 and 1.04, respectively (Fig. 2a). The reactivity ratios were both close to 1, further suggesting that the resultant polymer composition of Zn(II)/Pt(II) reflected the feeding

molar ratio of DPAZn(II)Ac/DPAPt(II)Ac in the polymerization process. In other words, the copolymerization of DPAZn(II)Ac/DPAPt(II)Ac proceeded randomly in an ideal manner.

To further demonstrate the copolymerization of DPAZn(II)Ac and DPAPt(II)Ac to obtain copolymers with controlled Zn/Pt ratios, their copolymerization was performed so that the monomer conversion rate exceeded 30%. As shown in Table S2 (ESI†), Zn2/Pt1 and Zn1/Pt1, which were prepared through the copolymerization of DPAZn(II)Ac and DPAPt(II)Ac with molar ratios of 2/1 and 1/1, respectively, exhibited Zn(II)/Pt(II) ratios consistent with the feeding monomer composition. Based on the monomer consumption of the polymerization, the degree of polymerization (DP) values of DPAZn(II)Ac and DPAPt(II)Ac were determined to be 24 and 12 for Zn2/Pt1, respectively, and they were determined to be 16 and 15 for Zn1/Pt1, respectively, under the assumption that the RAFT agents controlled the polymerizations well. It should be further noted that the obtained Zn2/Pt1 and Zn1/Pt1 exhibited unimodal molecular weight distributions with  $M_n = 3800$  and  $D = 1.132$ , and  $M_n = 4400$  and  $D = 1.115$ , respectively, as determined by GPC measurements using the PEG standard after removing the metal ions (Fig. 2c).

Nanoparticles were prepared using co-polymers as Legos blocks, as an extension of the obtained polymers. Nanostructures loaded with different metal ion species hold broad application potential because intermetallic catalytic nanomaterials have demonstrated distinct advantages over individual metallic nanomaterials.<sup>22,23,26</sup> However, different metal ion species cannot be incorporated into nanoparticles at a given ratio simply by mixing two metal ions at the intended molar ratio because metal ions have individual association constants. Regulating the metal composition requires some process to solve this limitation. Nanoparticles built by assembling polymers are assumed to have the same metal composition as the polymers. Thus, methods for building polymers with controlled metal compositions are advantageous for nanoparticle fabrication. In this evaluation, we selected plasmid deoxyribonucleic acid (pDNA) as a template for assembling co-polymers to form nanoparticles because DPAPt(II) and DPAZn(II) moieties are known to bind to DNA strands.<sup>19,22</sup> Nanoparticles with a unimodal size distribution were observed in DNA solutions mixed with either Zn2/Pt1 or Zn1/Pt1. Dynamic light scattering (DLS) was used to determine number average diameters of 31 nm and 74 nm, and polydispersity indices of 0.21 and 0.27, for Zn2/Pt1 and Zn1/Pt1, respectively, suggesting the successful preparation of polymer complexes with DNA (polyplexes) (Fig. 3a).<sup>19,27,28</sup> To further elucidate the polyplexes containing Zn(II) and Pt(II), polyplexes with Zn1/Pt1 were observed using scanning transmission electron microscopy (STEM). Note that we did not use staining agents based on heavy metal elements, such as

Table 1 Characterization of polymerization by  $^1\text{H}$  NMR. Molar compositions of DPAZn(II)Ac and DPAPt(II)Ac for the feed monomer ratio and polymer composition

	Feed monomer ratio (molar%)		Recovered polymer composition (molar%)		Conversion (%)	$f$	$F$	$F(f-1)/F$	$F^2/f$
	Zn	Pt	Zn	Pt					
Entry 1	84.7	15.3	84.6	15.4	16.4	5.48	5.52	4.48	5.56
Entry 2	59.4	40.6	58.7	41.3	16.8	1.42	1.46	0.419	1.50
Entry 3	36.0	64.0	34.9	65.1	15.7	0.534	0.563	-0.464	0.590
Entry 4	7.0	93.0	6.7	93.3	12.6	0.0714	0.0749	-0.928	0.0785

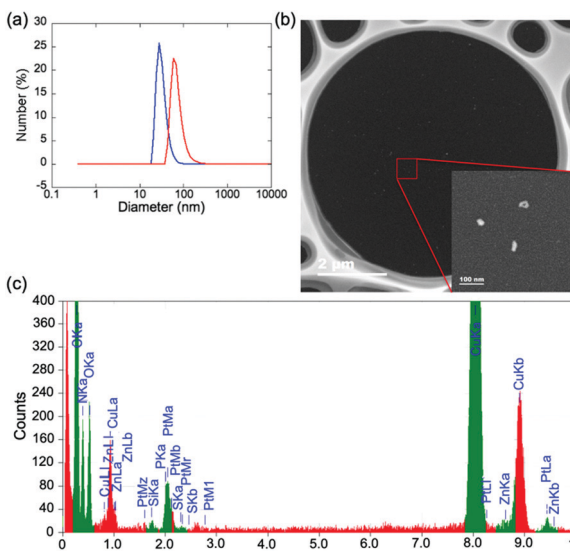


Fig. 3 Characterization of prepared polyplexes. (a) Size distribution of the polyplexes prepared from pDNA and Zn2/Pt1 (blue line), and Zn1/Pt1 (red line), detected by DLS measurements. (b) SEM images of the Zn1/Pt1 polyplexes and (c) representative EDS analysis results for the Zn1/Pt1 polyplexes.

uranyl acetate, which are typically used in the transmission electron microscopy (TEM) imaging of DNA and DNA polyplexes.<sup>27,28</sup> As shown in Fig. 3b, nanostructure images with sufficient contrast were successfully obtained, probably as a result of the platinum element clustering. Subsequently, the observed nanostructures were analyzed using energy-dispersive X-ray spectroscopy (EDS). Although the quantitative analysis of elements to determine the elemental composition of individual nanoparticles remains difficult because of the large differences between the signal thresholds of the elements, platinum and zinc signals were detected from the nanoparticles, as well as a phosphorus signal associated with DNA phosphates (Fig. 3c). This analysis confirmed that the nanoparticles were polyplexes containing Zn(II) and Pt(II). It should be noted that to the best of our knowledge, it is rare to successfully use STEM to observe and determine the elements of polyplexes at the scale of a nanoparticle, which would not have orderly structures like a crystal. These results further validated the currently proposed technique for constructing polymers, which is very promising for the fabrication of nanoparticles with well-defined and controllable metal-ion compositions.

In summary, we successfully polymerized DPAnZn(II)Ac and DPAnPt(II)Ac and achieved the random copolymerization of DPAnZn(II)Ac and DPAnPt(II)Ac. The controlled fabrication of random co-polymers is very advantageous; reducing the random copolymers of different metal complexes would be a feasible method to fabricate nano- and/or micro-scale metal alloys,<sup>14</sup> which have high catalytic activity. Controlling the metal composition of nano- and/or micro-scale structures cannot be achieved by simply considering the ratio of the feeding metal ions. Other well-thought-out strategies must be applied because the activation energies and speeds of the metal ion reductions vary across metal species. In our investigation, nanoparticles with different metal species were obtained using

copolymers with a controlled metal composition as the Lego blocks. Therefore, the proposed process could be extended to a novel methodology for fabricating intermetallic nanomaterials, which could potentially outperform materials fabricated using the current methods.

The authors appreciate Prof. T. Kawasaki and Mr S. Ohashi for kind help to mass spectrometry measurements. This work was financially supported by Grants-in-Aids for Early Carrier Scientists (JSPS KAKENHI Grant Number 20K15346 to S. O.) from Japanese Society of the Promotion of Science (JSPS).

## Conflicts of interest

There are no conflicts to declare.

## References

- Y. Yan, J. Zhang, L. Ren and C. Tang, *Chem. Soc. Rev.*, 2016, **45**, 5232.
- S. Rojas and P. Horcajada, *Chem. Rev.*, 2020, **120**, 8378.
- D. Baranov, G. Caputo, L. Goldoni, Z. Dang, R. Scarfiello, L. De Trizio, A. Portone, F. Fabbri, A. Camposeo, D. Pisignano and L. Manna, *Chem. Sci.*, 2020, **11**, 3986.
- S. Kim, A. U. Regitsky, J. Song, J. Ilavsky, G. H. McKinley and N. H. Andersen, *Nat. Commun.*, 2021, **12**, 667.
- S. Osawa, K. Kitanishi, M. Kiuchi, M. Shimonaka and H. Otsuka, *Macromol. Rapid Commun.*, 2021, **42**(16), 2100274.
- S. Osawa, R. Takahashi, R. Watanabe, S. Kubo and H. Otsuka, *RSC Adv.*, 2019, **9**(45), 26429.
- Y. S. Kim, R. Tamate, A. M. Akimoto and R. Yoshida, *Mater. Horiz.*, 2017, **4**, 38.
- R. Teshima, Y. Kawano, T. Hanawa and A. Kikuchi, *Polym. Adv. Technol.*, 2020, **21**, 3032.
- S. Furukawa and T. Komatsu, *ACS Catal.*, 2017, **7**, 735.
- T. Kawakami, A. Ebina, Y. Hosokawa, S. Ozaki, D. Suzuki, S. Hossain and Y. Negishi, *Small*, 2021, **17**, 2005328.
- R. Shunmugam and G. N. Tew, *J. Am. Chem. Soc.*, 2005, **127**, 13567.
- F. Freire, J. M. Seco, E. Quiñoa and R. Riguera, *J. Am. Chem. Soc.*, 2012, **134**, 19374.
- C. G. Hardy, J. Zhang, Y. Yan, L. Ren and C. Tang, *Prog. Polym. Sci.*, 2014, **39**, 1742.
- Q. Dong, Z. Meng, C.-L. Ho, H. Guo, W. Yang, I. Manners, L. Xu and W.-Y. Wong, *Chem. Soc. Rev.*, 2018, **47**, 4934.
- H. Zhang, Z. Zhou, X. Chen, B. Yu, Z. Luo, X. Li, M. A. Rahman and Y. Sha, *Macromolecules*, 2021, **54**, 9174.
- P. Suktanarak, S. Watchasit, K. Chitchak, N. Plainpan, K. Chainok, P. Vanalabhpata, P. Pienpinijtham, C. Suksai, T. Tuntulani, V. Ruangporvisuti and P. Leeladee, *Dalton Trans.*, 2018, **47**, 16337.
- E. C. M. Tse, D. Schilter, D. L. Gray, T. B. Rauchfuss and A. A. Gewirth, *Inorg. Chem.*, 2014, **53**, 8505.
- H. Zhao, P. Zhou, K. Huang, G. Deng, Z. Zhou, J. Wang, M. Wang, Y. Zhang, H. Yang and S. Yang, *Adv. Healthcare Mater.*, 2018, **7**, 1800296.
- S. Liu, D. Zhou, J. Yang, H. Zhou, J. Chen and T. Guo, *J. Am. Chem. Soc.*, 2017, **139**, 5102.
- A. Sarkar, R. Kumar, B. Das, P. S. Ray and P. Gupta, *Dalton Trans.*, 2020, **49**, 1864.
- R. Olivova, J. Kasparkova, O. Vrana, M. Vojtiskova, T. Suchankova, O. Novakova, W. He, Z. Guo and V. Brabec, *Mol. Pharmacol.*, 2011, **8**, 2368.
- S. Payra, S. Shenoy, C. Chakraborty, K. Tarafder and S. Roy, *ACS Appl. Mater. Interfaces*, 2020, 19402.
- M. Zhou, C. Li and J. Fang, *Chem. Rev.*, 2021, **121**, 736.
- F. R. Mayo and F. M. Lewis, *J. Am. Chem. Soc.*, 1944, **66**(9), 1594.
- M. Fineman and S. D. Ross, *J. Am. Chem. Soc.*, 1950, **5**(2), 259.
- D. Kim, J. Resasco, Y. Yu, A. M. Asiri and P. Yang, *Nat. Commun.*, 2014, **5**, 4948.
- S. Osawa, K. Osada, S. Hiki, A. Dirisala, T. Ishii and K. Kataoka, *Biomacromolecules*, 2016, **17**(1), 354–361.
- T. A. Tockary, W. Foo, A. Dirisala, Q. Chen, S. Uchida, S. Osawa, Y. Mochida, X. Liu, H. Kinoh, H. Cabral, K. Osada and K. Kataoka, *ACS Nano*, 2019, **13**, 12732.